

B Cleavage patterns of talin detected by anti-talin (C20) from different preparations of MEF

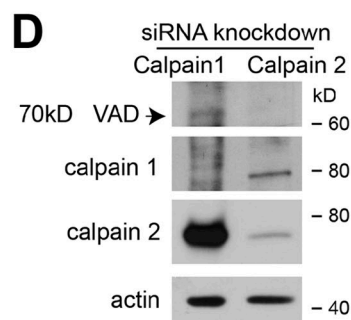
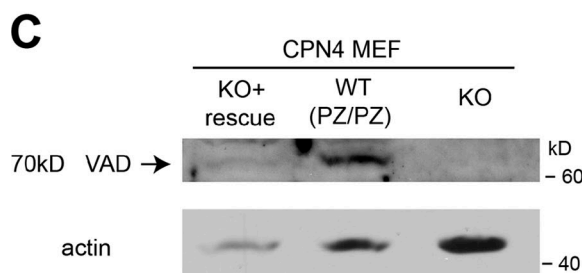
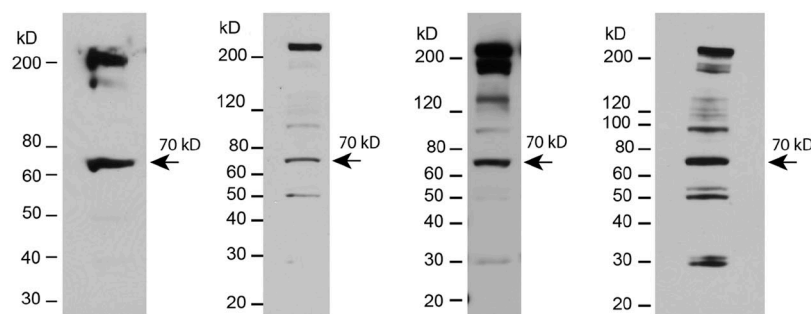


Figure S1. Conditional generation of the 70-kD C-terminal talin fragment in vivo. (A) The domain structure and the novel cleavage site of talin. Predicted cleavage at Ala 1903 exposes the free N terminus in order to allow arginylation by Ate1. The resulting 70-kD fragment contains vinculin- and actin-binding sites and a dimerizing domain (therefore referred to as the VAD fragment). The recognition epitopes for the two different talin antibodies (8d4 and C-20) used in this study are also indicated above. Note that talin contains multiple binding sites to vinculin and actin but only a few were illustrated here. Talin also contains multiple binding sites to integrin but only the one with the highest affinity is indicated here. Inside the VAD fragment region a low affinity integrin-binding site was also reported but is not shown. (B) Four representative immunoblots probed by anti-talin C20 showing the proteolytic cleavage patterns and the presence of the 70-kD VAD fragment in different preparations of confluent MEF cultures. The amount of 70-kD fragment varies in levels, from as low as 10% to surpassing that of the full-length talin in the cells, suggesting a multilevel regulation of this fragment's generation. The presence of other proteolytic fragments of talin suggests that additional types of regulatory processing of talin exist in vivo and may be dependent on conditions other than cell confluency. These fragments are invariably minor compared with the 70-kD band. (C) Representative immunoblots showing the level of the 70-kD talin VAD fragment in calpain-deficient calpain-4 knockout (CPN4 KO) cell line in comparison with the wild-type floxed cell line (PZ/PZ) and the rescue cell line (CPN4 KO + Rescue), in which recombinant calpain-4 was stably expressed. Actin was used as loading control. (D) Representative immunoblots showing the effects of stably knocked down calpain-1 or calpain-2 in MEF by retroviral vectors carrying calpain isoform-specific siRNAs. The levels of the VAD fragment, calpain-1, and calpain-2 were compared with actin as a loading control.

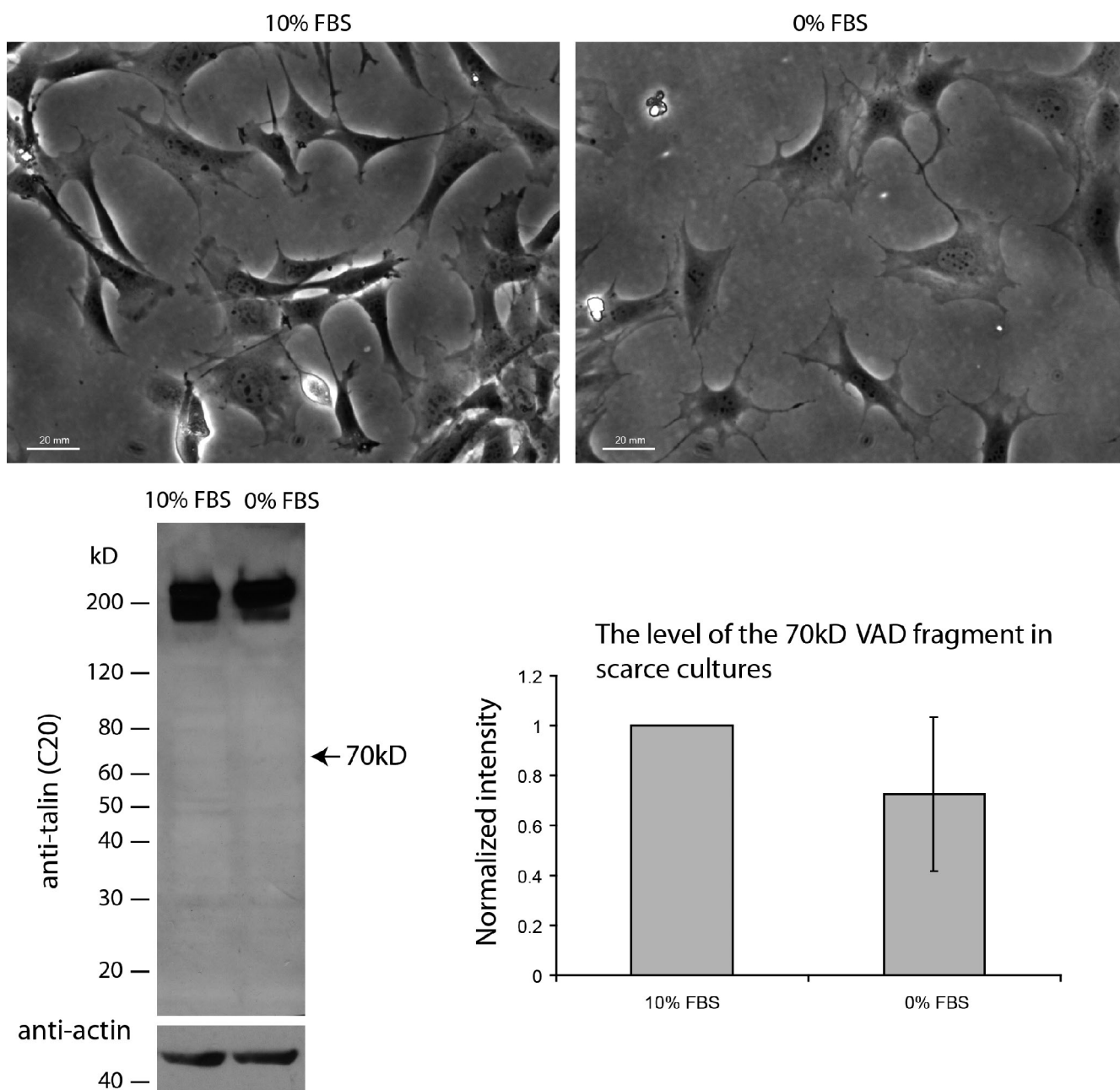


Figure S2. **Inhibition of cell motility and division by serum starvation treatment does not increase the level of the VAD fragment in scarce cell cultures.** Top: morphology of a scarce cell culture treated with the medium containing 10% or 0% FBS overnight. Polarized cells with lamella and cells undergoing division can be seen in 10% FBS medium but not in the serum-free medium. Bottom left: representative immunoblot showing the cleavage pattern of talin probed by anti-talin C20, with actin as a loading control. The expected position of the 70-kD VAD fragment is indicated by an arrow. Bottom right: quantification of the levels of the VAD fragment in scarce cells after serum starvation normalized to that in 10% FBS. Error bar represents SEM ($n = 3$).

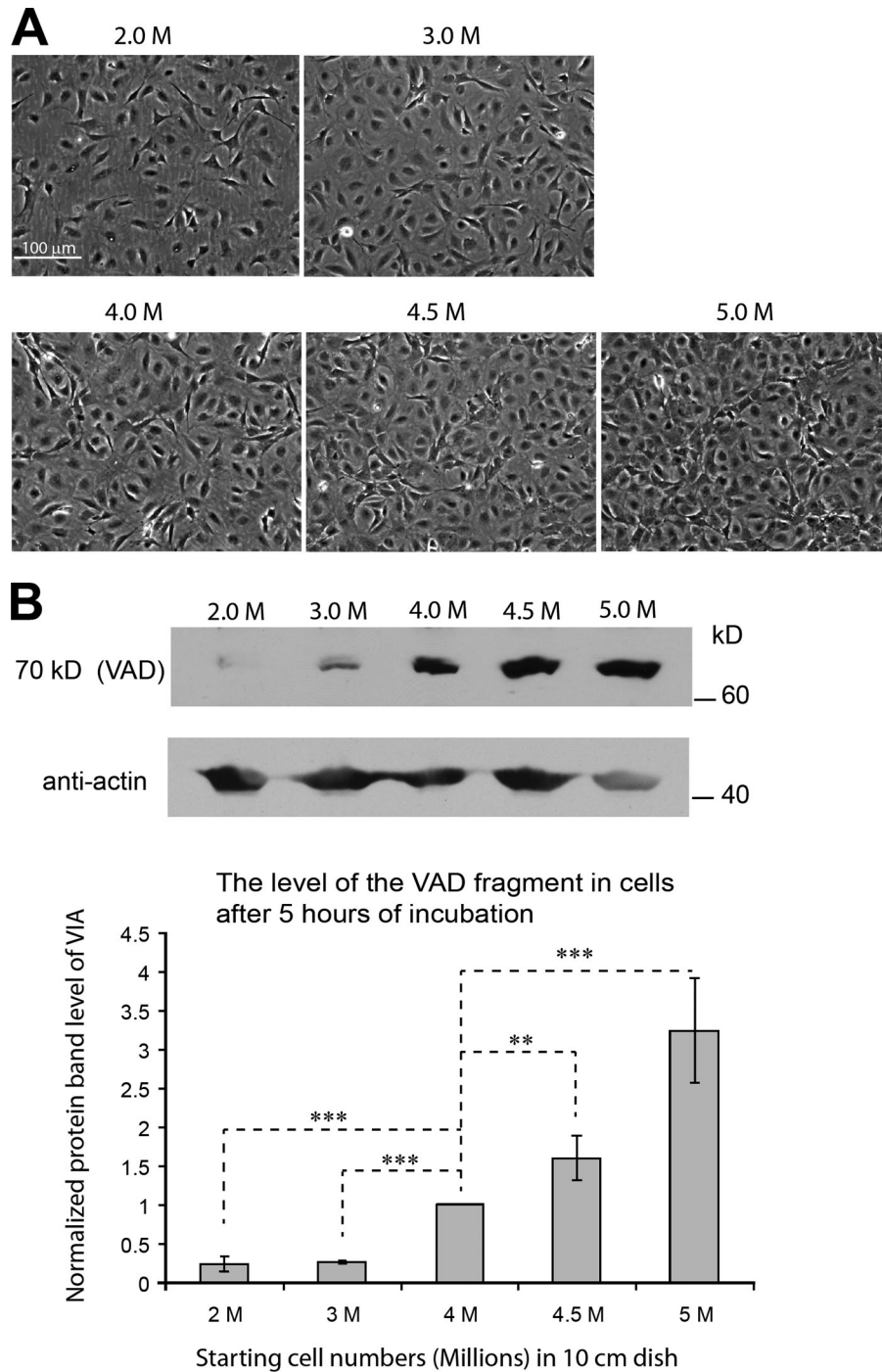


Figure S3. Level of the VAD fragment increases with the increase in cell density. The experiment was performed similarly to that described in the main text (Fig. 2), but cells were incubated for 5 h instead of overnight after plating at different densities. (A) Photos showing the morphology of the confluent cell cultures plated at increasing densities (numbers marked on the top of each photo represent cell number per 10 cm culture dish; “M” represents million) for 5 h. A steadily confluent monolayer was formed in cultures with 4 million and more cells in the dish. (B) Top: immunoblots showing the level of the 70-kD VAD fragment in the cells plated at different densities shown in A. Actin was used as a loading control. Bottom: quantification of the levels of the VAD fragment in the cells plated at different densities. Numbers represent the average band intensity of the VAD fragment adjusted to the loading control and normalized to the value of the sample with 4 million cells. Error bars represent SEM ($n = 3$). **, $P < 0.05$; ***, $P < 0.01$.

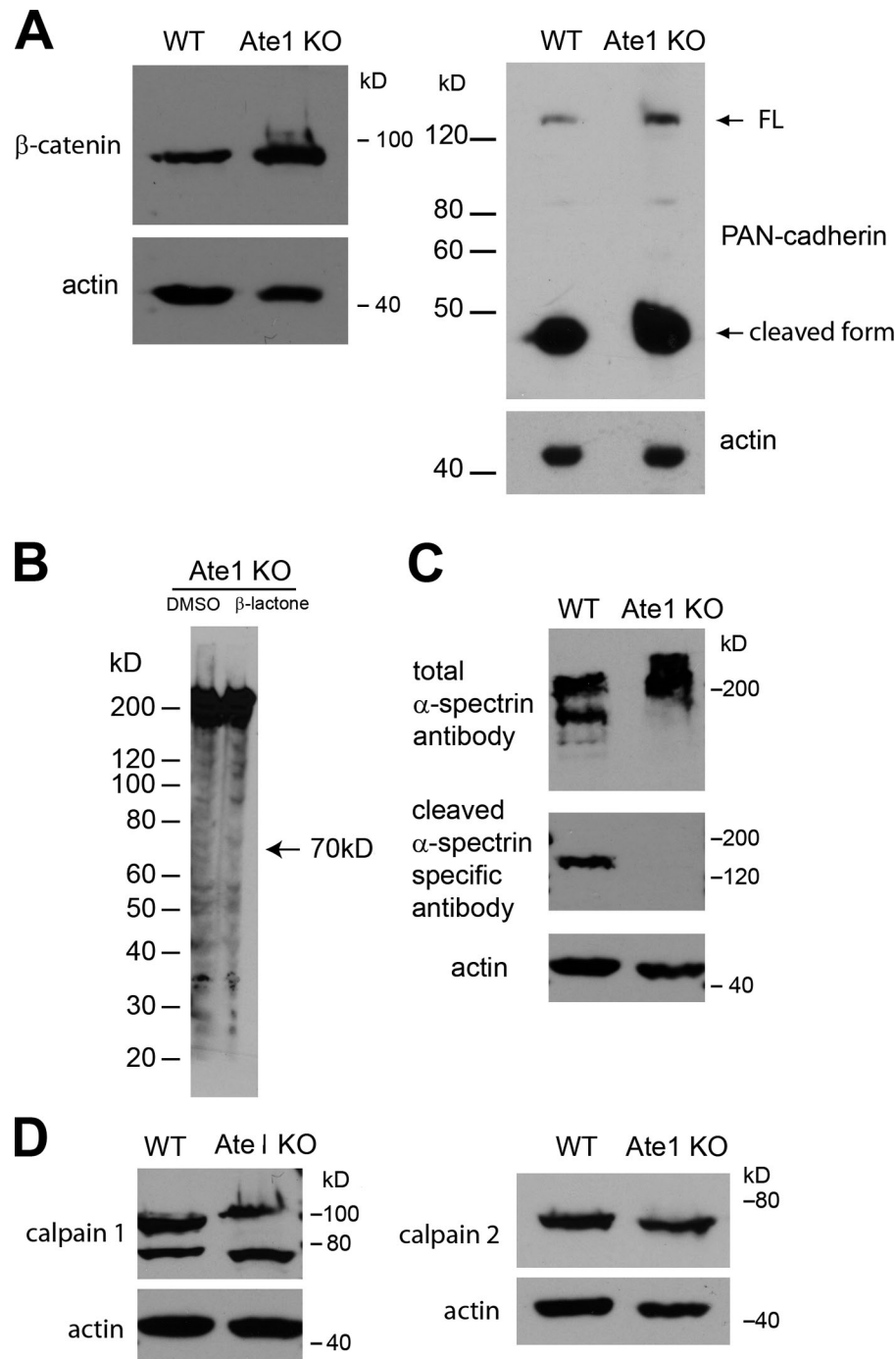
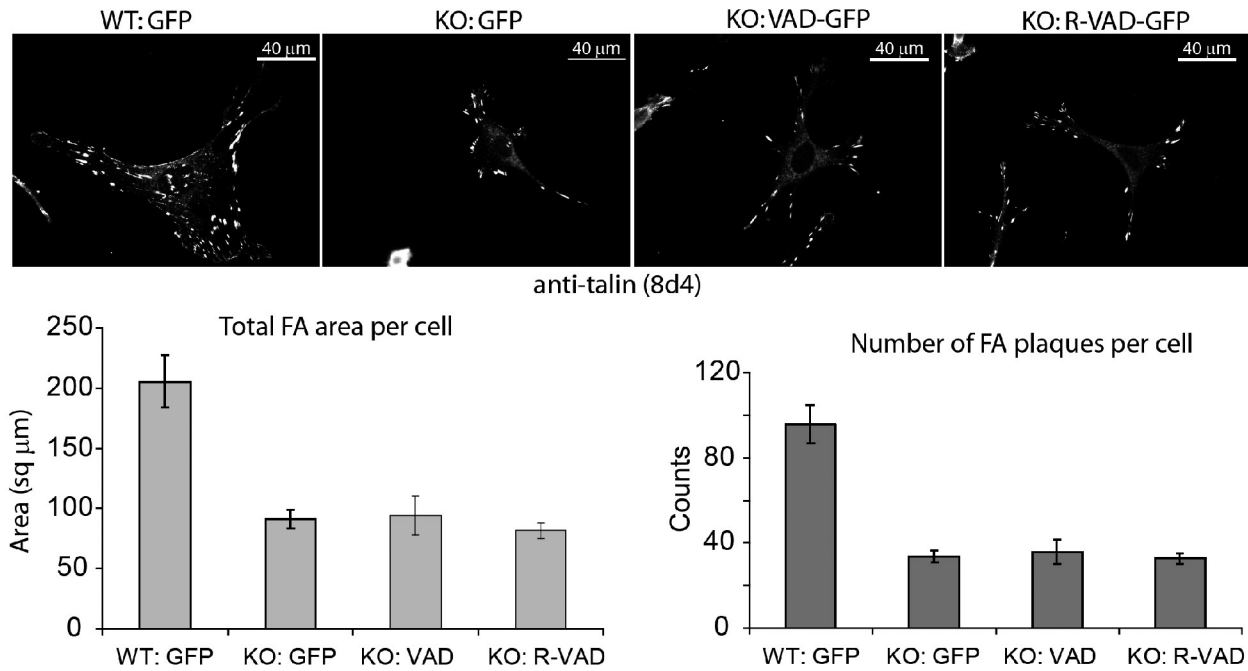


Figure S4. **Reduced calpain activity is likely responsible for the low level of the VAD fragment in Ate1 KO cells.** (A) Immunoblot comparison of the levels of β-catenin (left) and cadherin (stained with pan-cadherin antibody, right) in WT and Ate1 KO MEFs, with actin as a loading control. The top 130 kD representing full-length N-cadherin, as well as a cleavage product of around 45 kD are seen in the cadherin blot. Despite the weakened cell adhesion, the levels of both cadherin and β-catenin in Ate1 KO cells are not reduced compared with WT. (B) Immunoblots of Ate1 KO cell extracts from confluent cultures before (left) and after (right) treatment with the proteasome inhibitor β-lactone, probed with talin C20 antibody to detect talin's 70-kD fragment. The level of this fragment does not increase upon proteasome inhibition, suggesting that proteasome activity is not responsible for the low levels of this fragment in Ate1 KO cells. (C) Immunoblot with antibodies to α-spectrin and its calpain cleavage products, showing spectrin cleavage pattern in WT and Ate1 KO cells, with actin as a loading control. Calpain-dependent cleavage of spectrin occurs only in WT and not Ate1 KO cells, suggesting that calpain activity is reduced upon Ate1 knockout. (D) Immunoblot comparisons of the levels of calpain-1 (left) and calpain-2 (right) in WT and Ate1 KO cells, with actin as a loading control.

A

Focal adhesions (FA) in isolated cells visualized by epi-fluorescence microscopy

**B**

Focal adhesions in confluent cells visualized by TIRF-microscopy

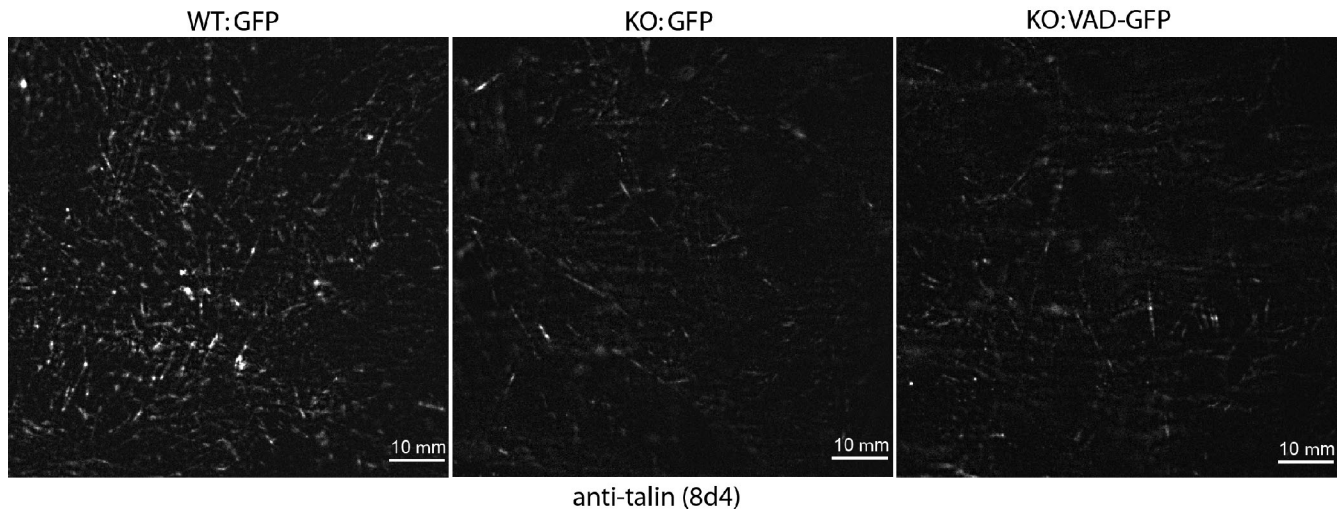


Figure S5. **Re-introduction of the VAD fragment into Ate1 KO cells does not rescue the focal adhesion defects.** (A) Top: representative images of scarce cells (WT and Ate1 KO) stably transfected with VAD-GFP, R-VAD-GFP, or GFP, and fluorescently stained with anti-talin 8d4 to visualize focal adhesions (FA). Bottom: quantification of the total focal adhesion area (left) and the total number of focal adhesion sites (right) in each cell, obtained by the analysis of images similar to those shown in the top panels. Error bars represent SEM ($n = 12$ for WT:GFP; $n = 16$ for KO:GFP; $n = 12$ for KO:A-VAD; $n = 31$ for KO:R-VAD). (B) Fluorescence images showing focal adhesions stained by anti-talin 8d4 in confluent cultures of WT and Ate1 KO cells transfected with GFP or VAD-GFP as indicated on the bottom of each image, visualized by total internal reflection fluorescence (TIRF) microscopy.